Ecological Indicators 181 (2025) 114390

Contents lists available at ScienceDirect

Ecological Indicators

journal homepage: www.elsevier.com/locate/ecolind

Original Articles

City-scale $PM_{2.5}$ removal by urban trees: validation of i-Tree eco and biomonitoring of $PM_{2.5}$-bound trace elements

Tzu-Hao Su [a,b,*], Chin-Sheng Lin [a,c], Chiung-Pin Liu [a]

[a] *Department of Forestry, National Chung Hsing University, Taichung City 402202, Taiwan*
[b] *Silviculture Division, Taiwan Forestry Research Institute, Taipei City 100060, Taiwan*
[c] *Environment Division, Agricultural Engineering Research Center, Taoyuan City 32061, Taiwan*

ARTICLE INFO

Keywords:
Air pollution
Dry deposition flux and velocity
Ecosystem services
Heavy metal pollution
Model calibration and validation
Urban forest

ABSTRACT

Urban trees play a critical role in mitigating fine particulate matter ($PM_{2.5}$) pollution through dry deposition, yet widely applied models such as i-Tree Eco remain insufficiently validated, often relying on single-species or short-term studies that overlook spatiotemporal variability. This study provides the first multi-species, spatiotemporal empirical validation of i-Tree Eco, based on leaf-surface $PM_{2.5}$ dry deposition measurements across five broadleaf tree species, three urban sites, and five time periods in Taiwan. On average, measured deposition was 33.91 μg m^{-2} h^{-1}, with i-Tree Eco underestimating measured deposition by an average of 7 %, indicating robust performance for broad-scale, multi-species, and spatiotemporal applications. Under low and stable wind conditions, discrepancies were primarily linked to the limited representativeness of ambient $PM_{2.5}$ data for tree-level environments, underscoring the need for localized air quality measurements to refine model accuracy. Species differences also influenced dry deposition fluxes, with *Bischofia javanica* Bl., characterized by its thick, leathery leaves, exhibiting values closest to the species mean. We further identified a $PM_{2.5}$ dry deposition saturation threshold (approximately 442 h), providing insights into removal dynamics not currently represented in i-Tree Eco. Elemental analysis revealed elevated concentrations of Fe, Cu, Zn, Pb, Cr and Ni at urban sites compared to the *peri*-urban area, despite similar $PM_{2.5}$ mass levels, highlighting the importance of $PM_{2.5}$-bound heavy metal assessment and the role of urban trees as biomonitors of atmospheric heavy metals. Collectively, these findings not only provide an empirical basis for calibrating the urban forest air pollution removal model i-Tree Eco, but also demonstrate the potential of urban trees as passive samplers of $PM_{2.5}$ and its associated bound pollutants, advancing both ecosystem service quantification and urban air quality management strategies.

1. Introduction

The air purification function provided by urban trees and forests is widely regarded as one of the most important ecosystem services in cities (Nowak, 2023). Among various air pollutants, particulate matter (PM) has attracted growing concern due to its adverse effects on human health. In particular, fine particulate matter ($PM_{2.5}$), with its small aerodynamic diameter and high inhalability, poses significant health risks because it can carry hazardous substances deep into the respiratory system (Feng et al., 2016; Kermani et al., 2021; Kong et al., 2018; Sosa et al., 2017). Trees can intercept PM on the surfaces of their leaves, branches, and trunks, thereby facilitating the removal of these particles from the atmosphere and contributing to improved air quality (Han et al., 2020; Vos et al., 2013). Accurately quantifying the $PM_{2.5}$ removal capacity of urban forests can enhance public awareness of the air quality benefits provided by urban vegetation. It also enables urban planners and decision-makers to better assess the contribution of different tree species to air purification, thereby informing more effective and needs-based urban forest management strategies (Gaglio et al., 2022).

To assess the $PM_{2.5}$ removal capacity of urban forests, two commonly used quantitative methods are eddy covariance and leaf extraction. The eddy covariance method operates at the canopy scale, estimating dry deposition fluxes by measuring vertical turbulent transport based on mass conservation principles (Baldocchi, 2003; Pallozzi et al., 2020). However, its application in urban settings is limited by fragmented forest distribution and heterogeneous surface roughness, which violate the assumption of homogeneous terrain and reduce spatial resolution (Pace et al., 2021). In contrast, the leaf extraction method operates at the

* Corresponding author at: Department of Forestry, National Chung Hsing University, Taichung City 402202, Taiwan.
E-mail address: thsu@tfri.gov.tw (T.-H. Su).

https://doi.org/10.1016/j.ecolind.2025.114390
Received 2 August 2025; Received in revised form 14 October 2025; Accepted 31 October 2025
Available online 13 November 2025

leaf scale and is widely used in urban environments. By collecting leaves and extracting surface-deposited PM through washing and vacuum filtration, this method directly reflects actual dry deposition. Despite its lower temporal resolution and labor-intensive process, this leaf-scale approach enables species-level comparisons and has been applied to investigate species-specific differences (Dzierżanowski et al., 2011; Sæbø et al., 2012; Song et al., 2015), canopy height effects (Hofman et al., 2014), variation with distance from roadways (Mori et al., 2015; Sgrigna et al., 2015), and differences between leaf surface regions, such as epicuticular wax and the lamina (Popek et al., 2013; Chen et al., 2024).

i-Tree Eco is a modeling tool developed by the U.S. Department of Agriculture Forest Service, based on the theoretical framework of the big leaf model. It estimates total leaf area using empirical formulas derived from tree survey parameters and calculates pollutant removal fluxes by combining pollutant-specific dry deposition velocities with local air quality monitoring data (Hirabayashi et al., 2022). Among urban forest models, i-Tree Eco is one of the most widely applied (Lin et al., 2019), with studies conducted across multiple spatial scales, including street scale (Riondato et al., 2020), neighborhood scale (Pace et al., 2018), city scale (Wu et al., 2019; Selmi et al., 2016; Riley et al., 2018), and regional scale (de Jalón et al., 2019; Nowak et al., 2013). However, for $PM_{2.5}$ removal, the model relies on dry deposition velocities derived from wind tunnel experiments conducted on a limited number of tree species. The average values obtained under different wind speed conditions for these few species are then uniformly applied across all species in the simulations, without accounting for the variability introduced by real-world microenvironmental conditions. In reality, PM deposition onto leaf surfaces is strongly influenced by microscale factors such as leaf position and specific leaf traits including surface roughness, trichome density, wax content, and wettability (Gaglio et al., 2022). As a result, there is a growing need for empirical validation to improve the accuracy of i-Tree Eco's estimations of air pollution removal and to strengthen its application in urban ecosystem service assessments (Pace et al., 2021).

Heavy metal contamination associated with airborne PM has become a critical focus in urban environmental studies. Due to their widespread distribution, urban trees are increasingly used as passive samplers or biomonitors for monitoring air pollutants, including the enrichment analysis of trace elements in PM and the assessment of spatial and temporal patterns at multiple scales. For example, Simon et al. (2011) analyzed nineteen heavy metals on both the surface and within the leaves of *Acer pseudoplatanus*, and found significantly higher concentrations in urban compared to rural sites. Similarly, Peachey et al. (2009) reported that metal accumulation in foliage decreased from city centers toward suburban areas, indicating that traffic emissions are a primary source of contamination. Norouzi et al. (2015) conducted a large-scale survey in Isfahan, Iran, using *Platanus orientalis*, and found that differences in metal concentrations between washed and unwashed leaves closely matched the spatial distribution of road dust containing iron (Fe), zinc (Zn), manganese (Mn), nickel (Ni), and copper (Cu), demonstrating the effectiveness of tree leaves as passive biomonitors. Moreover, the toxicity and health risks of $PM_{2.5}$ are not solely determined by particle mass concentration, but are strongly influenced by its chemical composition (Xie et al., 2017; Zheng et al., 2016). By integrating quantitative assessments of $PM_{2.5}$ retention with compositional analyses of harmful substances such as heavy metals, the ecological benefits of urban trees in improving air quality can be more comprehensively evaluated. In addition, this integrative approach may help reveal a hidden ecosystem service: the ability of urban vegetation to provide spatiotemporal information on pollutant characteristics, thereby supporting long-term environmental monitoring and urban planning.

With the increasing reliance on the i-Tree Eco model to estimate the air pollutant removal capacity of urban forests, field-based validation remains critical but has so far been limited. This study combined field measurements of leaf-surface $PM_{2.5}$ dry deposition across multiple tree species, sites, and time periods with simulations generated by the i-Tree Eco model. Measured deposition fluxes at different spatial and temporal scales were compared with model outputs to assess consistency. In parallel, the elemental composition of $PM_{2.5}$—including heavy metals and trace elements—was analyzed to identify spatial and temporal distribution patterns. The objectives were threefold: (i) to evaluate the accuracy of i-Tree Eco simulations against extensive empirical data, (ii) to identify sources of variation in deposition processes at the urban scale, and (iii) to explore potential improvements in model performance. Furthermore, the study investigated the biomonitoring potential of urban trees for trace elements associated with $PM_{2.5}$, thereby advancing understanding of their dual role in regulating air quality and providing environmental information.

2. Materials and methods

2.1. Experimental location, sampling sites, and sampled tree species

The study was conducted in Taichung City, Taiwan (24°7′ N, 120°40′ E), where three districts were selected along a north-to-south gradient: Nantun, Dali, and Wufeng (Fig. 1). These sites represent different levels of urban development. Nantun is the most densely populated district, characterized by heavy traffic flow. Dali lies on the urban fringe and is predominantly residential, whereas Wufeng is situated in a *peri*-urban area surrounded by agricultural land. An air quality monitoring station is installed within each site at a height of 12–15 m above ground, recording hourly data on $PM_{2.5}$ concentrations, wind speed, and rainfall. Within a 500–1000 m radius of each station, five commonly planted street tree species were selected for leaf-surface $PM_{2.5}$ sampling. These species include *Melia azedarach* L., *Koelreuteria henryi* Dummer, *Camphora officinarum* C. Bauhin *ex* Nees, *Bischofia javanica* Bl., and *Pongamia pinnata* (L.) G. Panigrahi. Tree species were selected as native species that are also widely planted as street trees in urban areas of Taiwan. The selection encompassed a variety of leaf traits, including differences in shape, size, texture, and leaflet arrangement.

2.2. Leaf sampling and study period

For each tree species within each sampling site, three individual trees were randomly selected from the available population as biological replicates ($n = 3$). From each tree, leaf samples were randomly collected at a height of 5 m above ground, covering both the inner and outer canopy as well as different orientations. Approximately 1000–1500 cm^2 of total leaf area was sampled per tree. Only healthy leaves without visible signs of pests or disease were collected. Samples were sealed in sealed plastic bags and transported promptly to the laboratory, where they were stored at 4 °C until further processing for particulate extraction. Sampling was conducted during the late autumn to early spring period, which is generally regarded as the air pollution season in Taichung City. A total of five sampling events were carried out on October 10, November 8, and December 29 in 2018, and on January 31 and March 21 in 2019. These sampling events are denoted as T1 through T5. The corresponding dry deposition duration, mean wind speed, and average $PM_{2.5}$ concentration for each site and time point are summarized in Table 1.

2.3. Leaf surface washing and filtration procedure for $PM_{2.5}$ collection

Each leaf sample was placed in a 1.5-L plastic container with 500 mL of deionized water and shaken with care to ensure adequate rinsing without damaging the leaves. After removing the leaves, the rinsate was first passed through a 100-μm stainless steel sieve to eliminate large debris and non-suspended particulate matter. The filtrate was then processed using a 47-mm magnetic filter funnel (No. 4242, Pall Corporation, East Hills, NY, USA) connected to a vacuum pump (V-500, Büchi Labortechnik AG, Flawil, Switzerland). Sequential filtration was

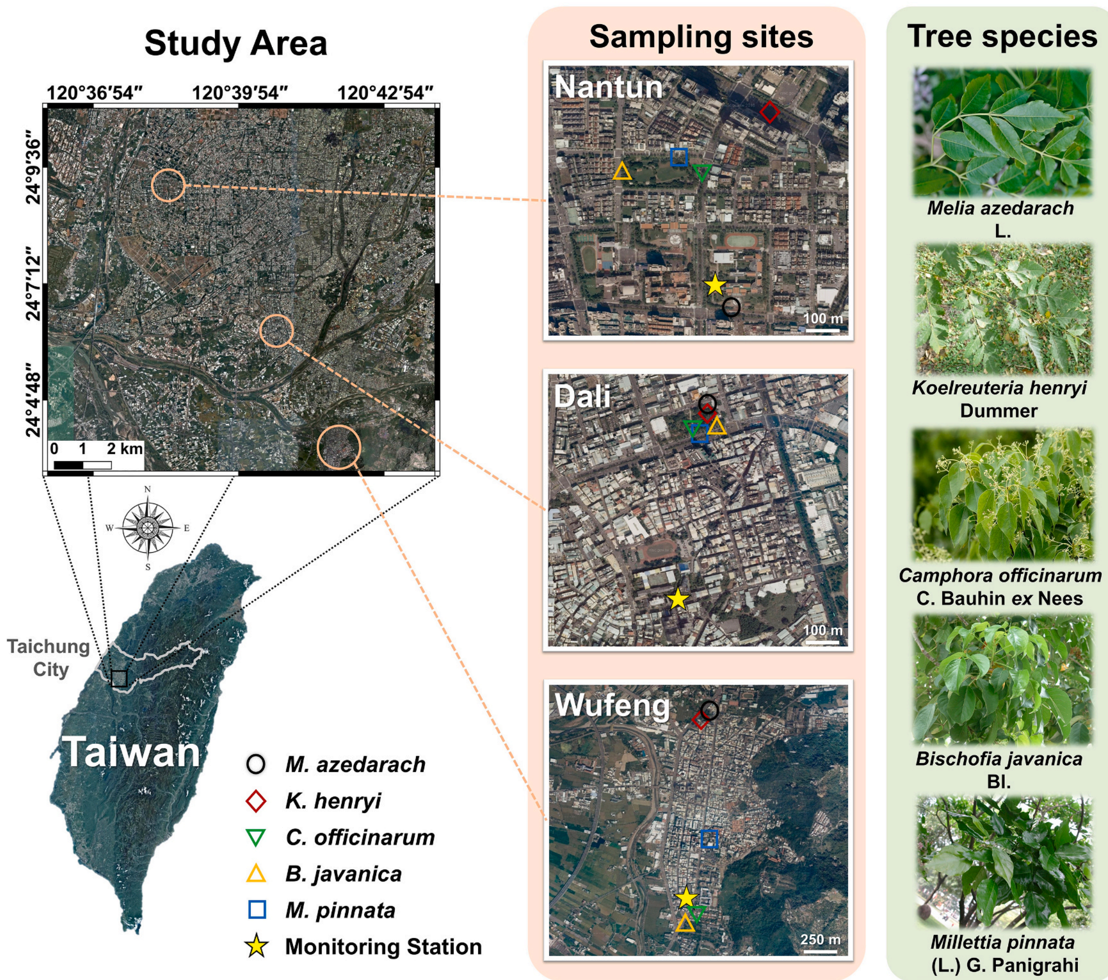

Fig. 1. Locations of sampling sites, tree species, and air quality monitoring stations within the study area.

Table 1
Dry deposition duration, mean $PM_{2.5}$ concentration, and wind speed at different sampling times and sites (Oct 2018–Mar 2019), based on data from air quality monitoring stations.

Parameters	Sampling site	T1 (10 Oct)	T2 (8 Nov)	T3 (29 Dec)	T4 (31 Jan)	T5 (21 Mar)
Duration of dry deposition (h)	Nantun	780	482	156	342	269
	Dali	539	485	161	345	271
	Wufeng	542	488	135	348	274
$PM_{2.5}$ concentration (μg m^{-3})	Nantun	20.52	21.63	6.70	27.25	32.48
	Dali	14.83	16.75	4.30	22.22	25.87
	Wufeng	16.79	21.43	8.61	23.84	26.36
Wind speed (m s^{-1})	Nantun	1.62	1.48	2.15	1.52	1.14
	Dali	1.85	1.28	1.75	1.33	1.13
	Wufeng	1.09	0.41	0.43	0.34	0.40

conducted using a cellulose filter (pore size: 2.5 μm; type 42, Whatman Corporation, Piscataway, NJ, USA) followed by a mixed cellulose ester (MCE) filter (pore size: 0.45 μm; GN-6, Pall Corporation, East Hills, NY, USA). Prior to use, filters were dried at 60 °C for 1 h and weighed using a microbalance with a precision of ± 0.01 mg (AP125WD, Shimadzu Corporation, Kyoto, Japan) under controlled humidity conditions (35 % to 40 %). A static eliminator (QUICK440A, Farnell Corporation, London, UK) was used to eliminate electrostatic interference and stabilize blank values. After filtration, the filters were dried and reweighed under the same conditions to determine post-filtration mass. The dry deposition of $PM_{2.5}$ on leaf surfaces was quantified by calculating the difference between the pre- and post-filtration weights of the MCE filter. In this study, $PM_{2.5}$ was defined as the insoluble particulate fraction within the size range of 0.45 to 2.5 μm collected from the leaf surface.

2.4. *Dry deposition flux and velocity of $PM_{2.5}$*

The quantified dry deposition of suspended particulates obtained through the rinsing and filtration procedures was further converted into flux values using the deposition area and deposition duration. The deposition area was defined as the total leaf surface area subjected to rinsing. After rinsing, the leaves were air-dried and scanned using a flatbed scanner. Leaf area was then measured using ImageJ software (National Institutes of Health, Bethesda, MD, USA). Deposition duration was determined based on hourly rainfall data from nearby air quality monitoring stations. It was calculated as the time elapsed since the last rainfall event considered sufficient to effectively remove deposited particulates from the leaf surface. According to previous studies, the rain interception threshold is estimated at 0.2 mm per unit leaf area (Wang et al., 2008), a value also adopted in the i-Tree Eco model for urban forest ecosystem services (Nowak et al., 2013). Since street trees typically have a leaf area index (LAI) of less than 5 (Gonzalez-Sosa et al., 2017; Rahman et al., 2015), and the sampled trees in this study did not exhibit dense canopies, a rainfall threshold of 1 mm (i.e., 0.2 × 5) was adopted. Any hourly rainfall event exceeding this threshold was considered sufficient to remove accumulated particulates, thereby marking the end of a dry deposition period and the start of a new one.

The dry deposition flux of $PM_{2.5}$ was then used to calculate the average leaf-surface dry deposition velocity over the dry deposition period using the following equation:

$$Vd = F/C$$

where Vd is the dry deposition velocity (m h^{-1}), F is the dry deposition flux (μg m^{-2} h^{-1}), and C is the mean ambient $PM_{2.5}$ concentration (μg m^{-3}) during the deposition period, obtained from the air quality monitoring station.

2.5. Comparison between i-Tree Eco estimates and field measurements

To compare the modeled and observed $PM_{2.5}$ dry deposition fluxes, the deposition velocity values specified in the i-Tree Eco model were used for simulation. According to Hirabayashi et al. (2022), the mean dry deposition velocities of $PM_{2.5}$ on leaf surfaces in i-Tree Eco are 0.03, 0.09, and 0.15 cm s^{-1} under wind speeds of 1, 2, and 3 m s^{-1}, respectively, which correspond to 1.08, 3.24, and 5.40 m h^{-1}. The respective resuspension rates under these wind conditions are 1.5 %, 3.0 %, and 4.5 %. Based on these values, hourly wind speed data from each air quality monitoring station were converted into hourly deposition velocity values using linear interpolation. The simulated hourly deposition flux was then calculated as the product of interpolated deposition velocity and ambient $PM_{2.5}$ concentration. Finally, the average of all hourly flux simulations during each dry deposition period was compared with the corresponding field measurements.

2.6. Leaf surface $PM_{2.5}$ loading saturation

To investigate whether a saturation threshold exists for the dry deposition of $PM_{2.5}$ on leaf surfaces, this study compiled dry deposition data across different tree species, time points, and sampling sites for analysis. Because leaf-surface $PM_{2.5}$ accumulation during the same dry deposition period may be influenced by differences in ambient concentration, direct comparisons of deposition amounts could be confounded by differences in pollutant levels. Therefore, the influence of concentration was normalized using the following equation:

$$D = A/C$$

where D is the dry deposition distance (m), A is the leaf-surface $PM_{2.5}$ dry deposition amount (μg m^{-2}), and C is the ambient $PM_{2.5}$ concentration (μg m^{-3}). The rate of change in deposition distance over time corresponds to the dry deposition velocity, which can be expressed as the slope of a graph with time on the x-axis and deposition distance on the y-axis. A positive slope indicates continued accumulation of particles on leaf surfaces, with steeper slopes representing faster deposition rates. When the slope approaches zero, the leaf surface is likely nearing saturation, and the accumulation rate has slowed substantially. A negative slope suggests net particle loss from the surface, potentially due to resuspension. This slope-based interpretation provides a useful indicator of the changing retention capacity of leaf surfaces and offers insight into deposition dynamics and potential saturation behavior across different species and environmental conditions.

2.7. $PM_{2.5}$ associated trace elements

Trace element analysis of leaf-deposited $PM_{2.5}$ was performed on the fraction retained on the 0.45 μm MCE filters. Each filter was placed in a digestion vessel containing 10 mL of diluted aqua regia, prepared by adding 55.5 mL of HNO_3 and 167.5 mL of HCl to ultrapure water and diluting to a final volume of 1 L. The digestion was conducted on a hot plate at 200 °C for at least 2 h. Once the filter was fully dissolved and the solution had been reduced to approximately 2–3 mL, it was allowed to cool and then diluted with ultrapure water to a final volume of 20 mL for elemental analysis. Blank filters were processed in the same manner and served as procedural blanks. Concentrations of nine trace elements, including aluminum (Al), chromium (Cr), Mn, Fe, Ni, Cu, Zn, lead (Pb), and cadmium (Cd) were determined using inductively coupled plasma–optical emission spectrometry (ICP-OES; Profile Plus, Leeman Labs, Lowell, MA, USA). The method detection limit for each element was 0.0001 mg L^{-1}. Calibration was performed using external standards (Merck, Darmstadt, Germany), and all analytical methods exhibited strong linearity ($R^2 > 0.9999$). Analytical precision was evaluated using relative standard deviation, which was required to be less than 3 % for high-concentration elements (> 0.1 mg L^{-1}) and less than 10 % for low-concentration elements (< 0.1 mg L^{-1}). The trace element contents in leaf-deposited $PM_{2.5}$ were expressed in μg g^{-1}.

2.8. Statistical analysis

For the dry deposition flux of $PM_{2.5}$, a three-way analysis of variance (ANOVA) was conducted to evaluate the main effects and interactions among three factors: sampling time (5 levels), site (3 levels), and tree species (5 levels). Post hoc comparisons were carried out using Tukey's honestly significant difference (HSD) test ($\alpha = 0.05$). As the original $PM_{2.5}$ flux data exhibited right-skewed distribution and heteroscedasticity, logarithmic transformation was applied to satisfy the assumptions of normality and homogeneity of variance required for ANOVA. To assess the potential saturation behavior of leaf surfaces over extended dry deposition periods, quadratic regression analysis was applied to the $PM_{2.5}$ deposition distance data for each tree species, with approximately 10 % of outlier points excluded to improve the reliability of saturation point estimation. For $PM_{2.5}$-bound trace element analysis, a two-way ANOVA followed by Tukey's HSD test ($\alpha = 0.05$) was performed to evaluate temporal and spatial differences. In addition to univariate comparisons, principal components analysis (PCA) was applied to the multi-element dataset to explore inter-element correlations and identify underlying compositional patterns. The suitability of the dataset for PCA was confirmed using the Kaiser–Meyer–Olkin test (threshold: 0.6) and Bartlett's test of sphericity ($p < 0.05$). For correlation analysis, replicate data were averaged for each tree species per time and site, yielding 75 samples across five species, five sampling times, and three sites. Spearman correlation analysis was then performed to assess the relationships between $PM_{2.5}$ dry deposition flux and ambient concentration, and between dry deposition velocity and wind speed. Spearman's rho (ρ) was used as the correlation coefficient. Statistical analyses were conducted using R (v. 4.3.2; R Development Core Team, 2023) and SPSS version 20 (IBM Corporation, Armonk, NY, USA; released 2011). Figures were generated using SigmaPlot 14.0 (Systat Software Inc., San Jose, CA, USA) and R.

3. Results

3.1. Effects of site, time, and tree species on $PM_{2.5}$ dry deposition flux

The dry deposition flux of $PM_{2.5}$ on leaf surfaces was significantly influenced by sampling time, site, and tree species, as revealed by a three-way ANOVA (Fig. 2). All main effects and two-way interactions were statistically significant ($p < 0.001$), while the three-way interaction was not. According to the interaction plot between tree species and site, species exhibited consistent performance trends across locations, with *M. azedarach* and *K. henryi* showing significantly higher fluxes, followed by *B. javanica* and *P. pinnata*, and with *C. officinarum* consistently exhibiting the lowest values. The time × species interaction likewise indicated that *M. azedarach* and *K. henryi*, which showed stronger $PM_{2.5}$ retention capacity, maintained relatively high and stable fluxes throughout the air pollution season, whereas *C. officinarum* remained consistently low across all time points, and *B. javanica* exhibited greater temporal variability. Overall, the back-transformed dry deposition flux values ranged from approximately 10 to 150 μg m^{-2} h^{-1} among species, with interspecific differences within the same

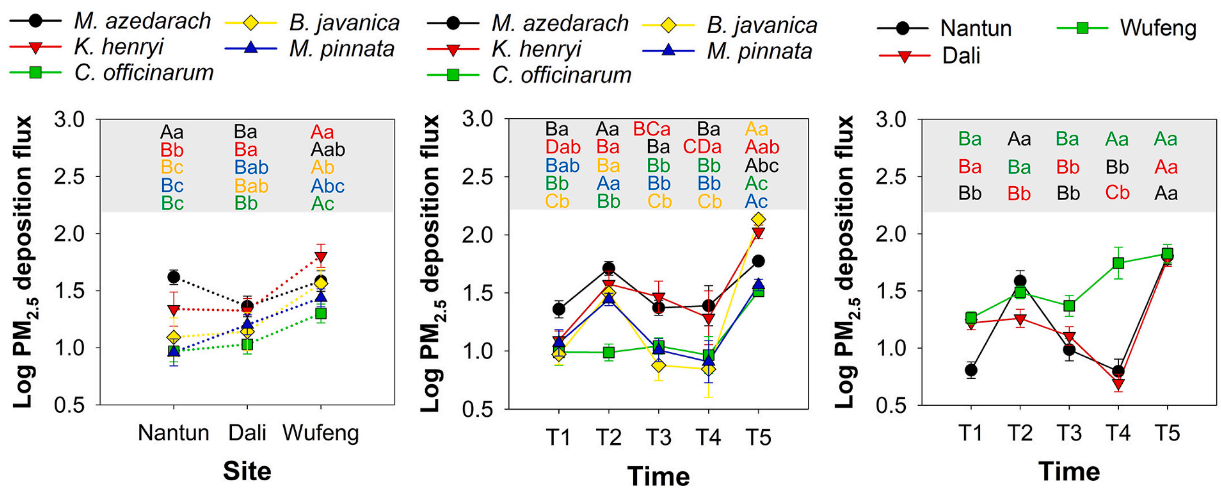

Fig. 2. Results of the three-way ANOVA on leaf-surface $PM_{2.5}$ dry deposition fluxes. The three-way interaction was not significant, and only significant two-way interactions are shown. Data are presented as mean ± standard error. Source data: $PM_{2.5}$ dry deposition flux (μg m^{-2} h^{-1}). Uppercase and lowercase letters in matching colors indicate significant differences in horizontal and vertical comparisons, respectively ($\alpha = 0.05$, Tukey's HSD test).

site or time point reaching up to 3- to 6-fold. In terms of spatiotemporal variation, the Wufeng site generally exhibited higher fluxes than the other two sites, peaking at T5 and showing an overall increasing trend throughout the observation period. In contrast, fluxes at the Nantun and Dali sites varied more markedly over time, both showing distinct troughs at T4 and relatively higher values at T2 and T5.

3.2. Field measurements and i-Tree Eco estimates of $PM_{2.5}$ dry deposition flux

The $PM_{2.5}$ dry deposition flux simulated by i-Tree Eco generally followed the temporal trends observed in field measurements at both the Nantun and Dali sites. However, at Nantun, the model substantially overestimated the flux at T4, reaching approximately seven times the

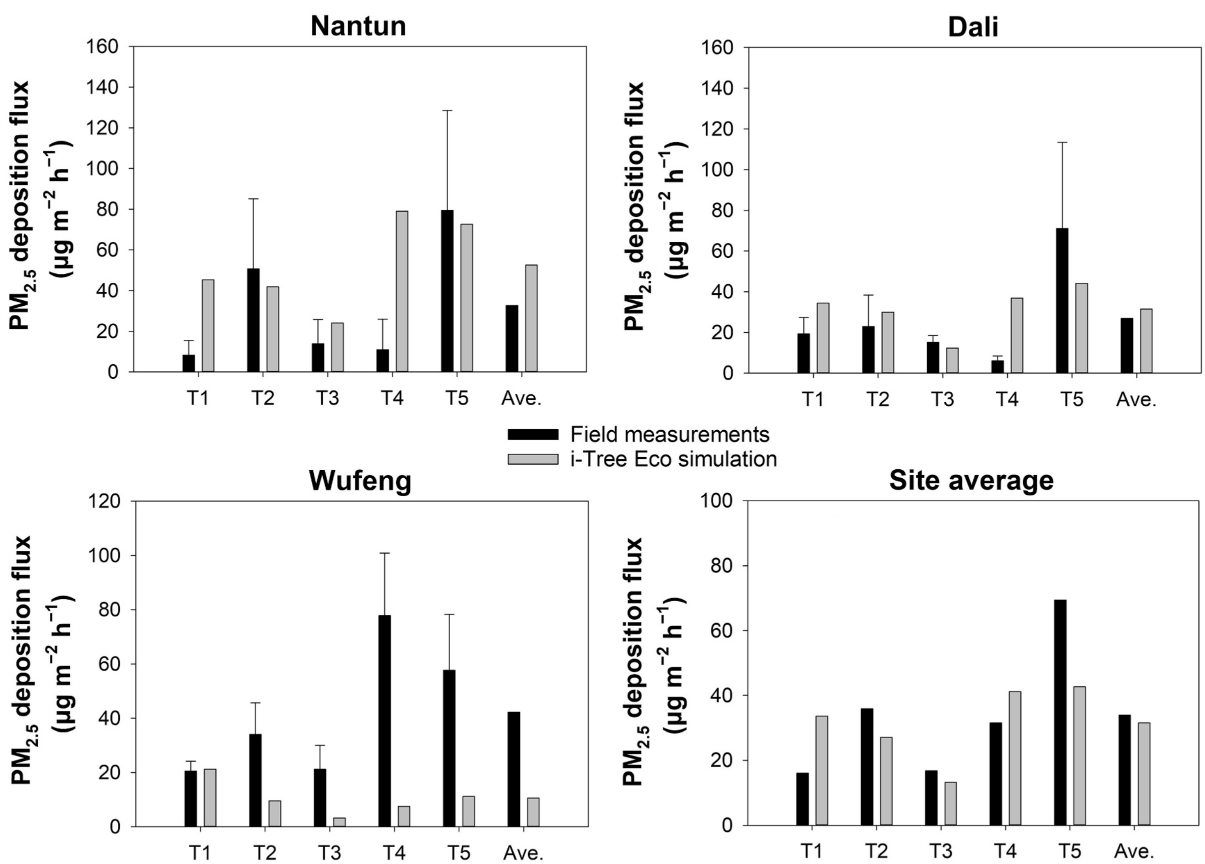

Fig. 3. Comparison between measured and i-Tree Eco simulated $PM_{2.5}$ dry deposition fluxes on leaf surfaces. For each site, measured values are presented as mean ± standard deviation for five tree species. At each sampling time, the site average was calculated as the mean value across the three sites, and "Ave." denotes the overall mean over sampling periods T1–T5.

measured value and resulting in a mean flux across time points that was about 38 % higher than the observed average. At the Dali site, the simulated fluxes were relatively close to the observed values overall, with only about a 15 % difference in the mean. In contrast, the Wufeng site exhibited markedly higher measured fluxes at T4 compared to the other two sites, reaching 7–13 times greater. Meanwhile, the simulated fluxes at Wufeng remained consistently lower than the measured values throughout the monitoring period, with the maximum discrepancy reaching up to 11-fold. Overall, despite site- and time-specific over- and underestimations, the average simulated flux across all conditions was 31.53 μg m^{-2} h^{-1}, which was close to the measured average of 33.91 μg m^{-2} h^{-1}, representing a difference of only about 7 % (Fig. 3).

3.3. Correlation analysis between dry deposition variables and environmental factors

The $PM_{2.5}$ dry deposition flux on leaf surfaces across different tree species exhibited a significant weak-to-moderate positive correlation with ambient $PM_{2.5}$ concentrations measured at the monitoring station ($\rho = 0.379$, $p < 0.001$), indicating that higher ambient concentrations were generally associated with increased leaf surface $PM_{2.5}$ deposition. The data also showed a divergent distribution pattern. Notably, *P. pinnata* and *C. officinarum* exhibited relatively limited increases in deposition flux under high $PM_{2.5}$ concentrations, resulting in a marked reduction in dry deposition velocity (Fig. 4**a**). In addition, the dry deposition velocity on leaf surfaces showed a low, non-significant negative correlation with wind speed recorded at the station ($\rho = -0.207$, $p = 0.075$), which contrasts with the trend assumed in the i-Tree Eco model, where deposition velocity increases with wind speed. Even under near-calm wind conditions (< 0.5 m s^{-1}), deposition velocities still ranged from 0.5 to 6.5 m h^{-1}. Overall, no clear interspecific differences were observed in the relationship between wind speed and leaf surface $PM_{2.5}$ dry deposition velocity (Fig. 4**b**).

3.4. Saturation patterns of $PM_{2.5}$ dry deposition on leaf surfaces

The results of $PM_{2.5}$ dry deposition distance showed that all tree species exhibited a stable increase during the initial phase of deposition. At the maximum deposition duration of 780 h, a decline in deposition distance was observed across all species. Among the tested species, *M. azedarach* showed the longest saturation time, reaching up to 530 h, and maintained relatively higher deposition distances throughout the period. In contrast, *C. officinarum* exhibited consistently lower deposition distances, with a poor fit to the regression model ($R^2 = 0.15$). Based on the averaged results across species, the saturation point occurred at approximately 442 h ($R^2 = 0.54$), with the deposition trend prior to saturation closely resembling that of *B. javanica* (Fig. 5).

3.5. Spatiotemporal variation in atmospheric $PM_{2.5}$-bound trace element concentrations

Cd concentrations were consistently below the detection limit in all $PM_{2.5}$ samples and were therefore excluded from further analysis. Among the detected trace elements, Fe and Al exhibited the highest concentrations, reaching up to 30000–40000 μg g^{-1}. Zn and Cr followed, with maximum levels around 6000–8000 μg g^{-1}, while Mn, Pb, and Cu were generally lower, with peak concentrations ranging from approximately 400 to 600 μg g^{-1}. Ni was the least abundant, with a maximum concentration of only about 100 μg g^{-1}. In terms of temporal variation, most elements in the Nantun site showed a bimodal distribution, with elevated concentrations during T1 and T3/T4. At the Dali site, Al, Fe, Mn, and Ni exhibited trends similar to those in Nantun, while Cu, Zn, and Cr showed a gradual decline over time. Pb was generally low and stable throughout the monitoring period, with an increase observed at T2. In Wufeng, most elements showed a decreasing trend over time, while Mn exhibited a relatively high concentration at T3. Ni levels remained consistently low (< 50 μg g^{-1}) with no significant temporal variation. Regarding spatial distribution, notable regional differences in trace element concentrations were primarily observed from T1 to T4, with generally higher levels recorded in Nantun and Dali compared to Wufeng. Ni also showed a significant difference at T5, with elevated concentrations in Nantun. Overall, trace element concentrations in $PM_{2.5}$ across the study area in Taichung City exhibited a general urban-to-peri-urban decreasing gradient, with T1, T3, and T4 representing periods of relatively higher concentrations (Fig. 6).

3.6. Principal component analysis of atmospheric $PM_{2.5}$-bound trace elements

In the PCA of trace elements in atmospheric $PM_{2.5}$, three principal components with eigenvalues greater than 1 were extracted based on the average concentrations of trace elements across different tree species, regions, and time periods. The first component was associated with multiple elements, including Fe, Cu, Zn, Pb, and Cr, and accounted for approximately 45.0 % of the total variance. The second was primarily related to Mn and Al, explaining around 19.8 % of the variance, while the third was mainly associated with Ni, contributing approximately 12.6 %. Together, these three components explained about 77.4 % of the

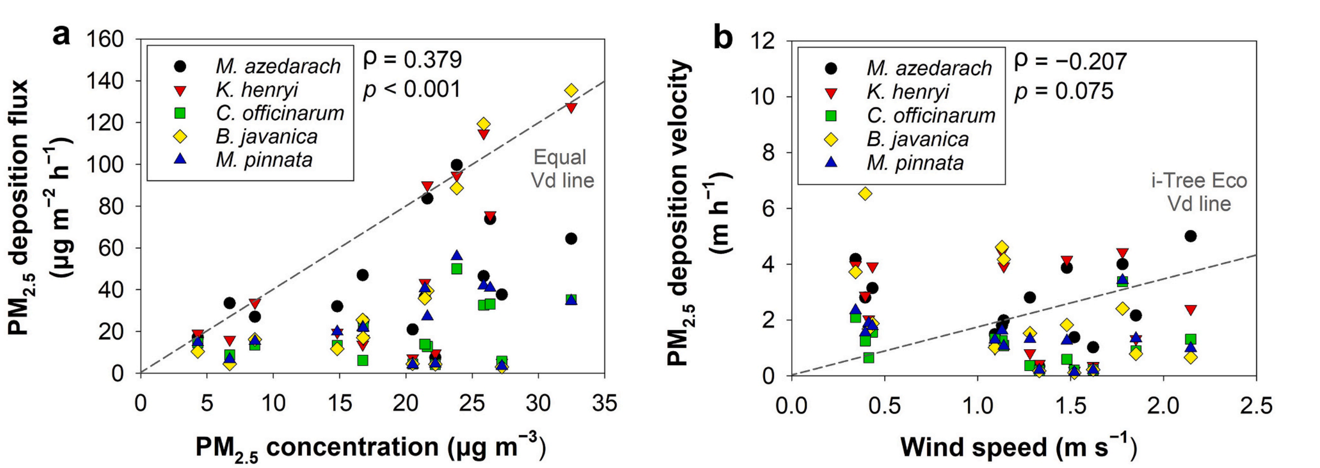

Fig. 4. Spearman correlation plots between (a) $PM_{2.5}$ dry deposition flux and ambient concentration, and (b) $PM_{2.5}$ dry deposition velocity and wind speed. ρ denotes the correlation coefficient. Each data point represents the mean of three replicates per tree species within each sampling time and site ($n = 75$). The “Equal Vd line” represents a constant deposition velocity (Vd = flux/concentration), while the “i-Tree Eco Vd line” indicates model-predicted $PM_{2.5}$ dry deposition velocities under different wind speeds.

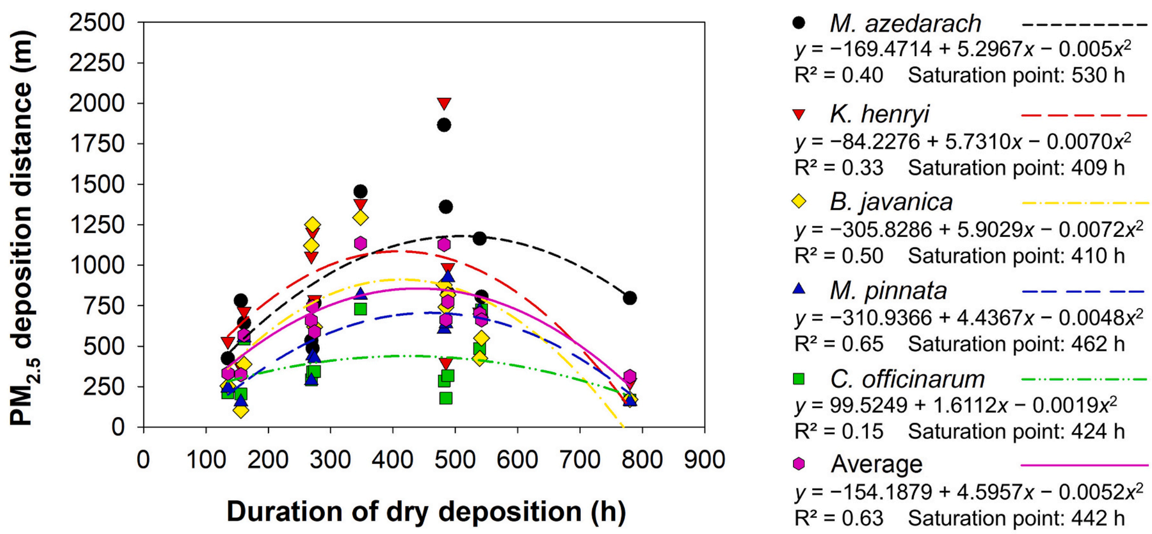

Fig. 5. Quadratic regressions between $PM_{2.5}$ dry deposition distance and dry deposition duration for each tree species. Each data point represents the mean of three replicates per species ($n = 15$ per species; total $n = 75$). Purple hexagonal points indicate the average values of the five species at the same deposition duration. The saturation point is defined as the deposition duration corresponding to a zero slope on the quadratic regression curve. (For interpretation of the references to colour in this figure legend, the reader is referred to the web version of this article.)

total variance, summarizing the major patterns in the dataset (Table 2).

4. Discussion

4.1. City-scale $PM_{2.5}$ deposition flux variation

Significant interactions between species and temporal or spatial factors indicate that $PM_{2.5}$ dry deposition fluxes on leaf surfaces vary temporally and spatially in a species-specific manner. Most previous studies emphasized interspecific comparisons; however, our results indicate that at single time points or locations may bias assessments of species performance. For example, Chen et al. (2017) found that species such as *Catalpa speciosa* and *Amygdalus triloba* exhibited significantly higher $PM_{2.5}$ interception during summer and autumn, yet their performance declined markedly in late spring. Zhang et al. (2017) similarly reported substantial monthly variation in *Pinus tabuliformis*. Lu et al. (2018) demonstrated that retention capacity varied by species, site, and month in a year-long urban study. Such variation partly reflects seasonal changes in leaf micromorphology—such as wax layers and trichomes—that influence particle adherence (Wang et al., 2013; Santunione et al., 2024). Therefore, multi-temporal, multi-site monitoring is essential for accurate species-level evaluation. Supporting this, Sæbø et al. (2012) found that the same species showed distinct PM retention across sites and years, and cluster analysis identified groups with consistently high retention potential.

The lack of a significant three-way interaction indicates that all species exhibited a similar spatiotemporal trend in $PM_{2.5}$ dry deposition. Notably, the Wufeng site and T5 period showed relatively higher deposition fluxes, suggesting that trees can serve as effective bioindicators of $PM_{2.5}$ distribution. High deposition fluxes may result from increased dry deposition velocity and/or elevated ambient concentrations. Wind speed is a key factor influencing deposition velocity, as higher wind speeds provide greater kinetic energy to enhance particle impaction on leaf surfaces (Freer-Smith et al., 2004). Although average wind speeds at the Wufeng station were low, near-surface airflow dynamics may differ from station records. Moreover, the combination of low ambient $PM_{2.5}$ concentrations and high deposition fluxes at Wufeng suggests the presence of localized emission sources not captured by conventional monitoring networks. These findings underscore the pronounced spatiotemporal heterogeneity of $PM_{2.5}$ dry deposition in urban environments and the need for fine-scale, cross-species monitoring to strengthen tree-based biomonitoring.

4.2. Modeling and field validation of $PM_{2.5}$ dry deposition flux

Comparison of field-measured $PM_{2.5}$ dry deposition fluxes with i-Tree Eco estimates revealed clear spatial discrepancies. The model performed well in Nantun and Dali but consistently underestimated fluxes in Wufeng (except T1), suggesting limitations in *peri*-urban settings. As i-Tree Eco relies on wind speed and $PM_{2.5}$ concentration as key inputs (Hirabayashi et al., 2022), the nearly calm rooftop wind speeds recorded at Wufeng are unlikely to explain the bias, since weak winds also prevail near the ground due to building obstruction (Adamek et al., 2017). Instead, the underestimation is more likely linked to unrepresentative concentration data. $PM_{2.5}$ is typically higher at lower building levels than rooftops (Wu et al., 2014), and the Wufeng station was farther from sampled trees than those at the other sites, further reducing its relevance. These results highlight that model performance is sensitive to monitoring height and spatial coverage, underscoring the need for representative $PM_{2.5}$ data and closer alignment between monitoring inputs and modeled vegetation areas.

i-Tree Eco has been widely applied to estimate pollutant removal at local (street or neighborhood) scales (Fares et al., 2020; Riondato et al., 2020), as well as at broader city or regional scales (Nowak et al., 2013; Wu et al., 2019). However, empirical validations of its modeling performance remain limited. One such example is the study by Pace et al. (2021), who employed a leaf surface filtration method similar to that used in our study to compare observed $PM_{2.5}$ deposition on *Quercus ilex* with i-Tree Eco estimates, reporting model underestimations ranging from 6- to 20-fold. Even when limiting deposition velocity inputs to broadleaved species, underestimations of 2.2–7.2 times remained. Given that their sampling was restricted to a single species and a single time point, the results highlight the need for long-term, site-specific parameter validations to improve model reliability. In support of this, previous studies have shown that $PM_{2.5}$ removal capacity can vary by orders of magnitude among tree species, with especially large differences observed between conifers and broadleaves (Liang et al., 2016; Sæbø et al., 2012; Zhang et al., 2020). Gaglio et al. (2022) further emphasized that species-specific leaf traits, age, and structural features—along with their interactions with rainfall-driven wash-off and resuspension—can significantly affect deposition estimates. They also noted that inconsistencies in leaf washing procedures prior to vacuum filtration may

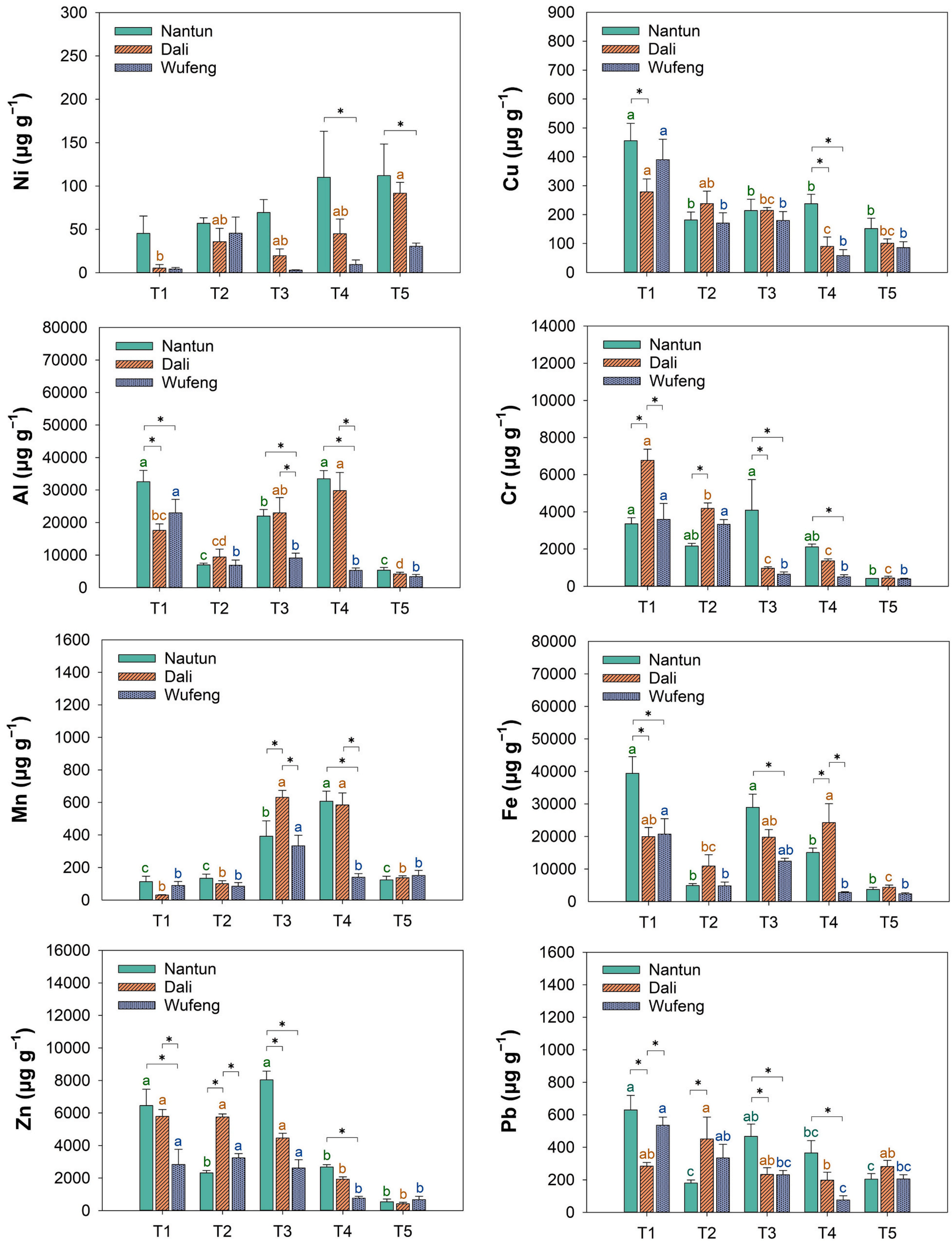

Fig. 6. Contents of $PM_{2.5}$-bound trace elements estimated via biomonitoring. Data are presented as mean ± standard error of five tree species. Significant spatial differences are indicated by asterisks, and significant temporal differences are indicated by different lowercase letters (α = 0.05, Tukey's HSD test).

Table 2
Principal component analysis (PCA) of atmospheric $PM_{2.5}$-bound trace element concentrations. Data represent species-averaged values within each site and sampling time. Factor loadings are from the rotated component matrix, with values greater than 0.6 shown in bold.

Variable	Principal component loading		
	PC1	PC2	PC3
Fe	**0.863**	0.197	−0.179
Cu	**0.799**	−0.214	0.218
Zn	**0.799**	−0.217	−0.136
Pb	**0.737**	−0.110	0.445
Cr	**0.649**	−0.468	−0.077
Al	0.496	**0.759**	−0.185
Mn	0.208	**0.852**	−0.268
Ni	0.010	0.498	**0.774**
Eigenvalue	3.604	1.583	1.007
Total variance (%)	45.046	19.784	12.590
Cumulative variance (%)	45.046	64.830	77.420

introduce additional measurement uncertainty. Therefore, improving the accuracy of $PM_{2.5}$ deposition modeling across tree species requires both the refinement of species-specific parameters and the standardization of experimental protocols.

Our findings align with these observations. Substantial standard deviations in observed $PM_{2.5}$ deposition fluxes across tree species were evident during the T5 period, when ambient $PM_{2.5}$ concentrations were relatively high, further underscoring the sensitivity of i-Tree Eco estimates to species-specific input values. In terms of spatial scale, the discrepancy between modeled and observed $PM_{2.5}$ dry deposition fluxes was notably smaller at the city level than at individual sites. Moreover, the close match between long-term observed averages and model outputs suggests improved model performance when applied across broader spatial and temporal scales. This indicates that i-Tree Eco is better suited for large-scale urban assessments of $PM_{2.5}$ removal by urban forests, whereas its application at neighborhood or street levels may introduce greater uncertainties. Although i-Tree Eco is a widely used integrated model, it currently does not support user-level adjustment of dry deposition parameters. Nevertheless, field measurements can provide essential empirical data for post-validation and model calibration. Such site-based observations help clarify the model's applicability across different species, temporal periods, and spatial scales, thereby improving simulation accuracy. Furthermore, as more field datasets become available—particularly those incorporating microclimatic variables and $PM_{2.5}$ concentration dynamics—they could serve as valuable references for refining deposition-related coefficients and enhancing the model's reliability under diverse urban and *peri*-urban conditions.

4.3. Dry deposition velocity and its environmental correlates

The dry deposition flux of $PM_{2.5}$ on leaf surfaces typically increases with ambient concentrations. However, when deposition velocity is unstable, this relationship may weaken. During the air pollution season in Taichung, characterized by low and stable wind speeds, a moderate but significant positive correlation was found between ambient $PM_{2.5}$ and deposition flux. High fluxes occurred only when ambient concentrations were elevated. Comparable trends have been observed in studies near roadways (Mori et al., 2015; Sgrigna et al., 2015) or under high PM exposure (Lu et al., 2018), where enhanced particle interception by leaves was reported. These observations emphasize the role of trees in capturing airborne pollutants during severe pollution episodes, thereby contributing to air quality regulation. Despite this, scatterplots of flux versus concentration revealed generally low deposition velocities, especially at high concentrations, implying reduced deposition efficiency under heavy pollution loads. Such a pattern is consistent with meteorological conditions associated with high-pressure systems during Taichung's fall and winter, where poor atmospheric dispersion and low wind speeds allow PM to remain suspended (Chen et al., 2023). Numerous studies have similarly noted negative correlations between wind speed and $PM_{2.5}$ concentrations, with elevated pollution levels commonly recorded during calm periods (Askariyeh et al., 2020; Fang et al., 2017; Wang et al., 2018).

Atmospheric conditions influence PM dry deposition on foliage through two primary mechanisms: by affecting ambient PM levels and by directly altering deposition dynamics (Cai et al., 2017). Wind speed, for instance, can disperse $PM_{2.5}$ and reduce its concentration near vegetation but may also cause wind-driven resuspension of particles already deposited on leaf surfaces (Xu et al., 2020). Conversely, stronger winds can provide greater kinetic energy to particles, promoting their contact with leaf surfaces and thereby enhancing deposition velocity (Chen et al., 2012; Mohan, 2016). These opposing effects underscore the dual role of wind in regulating dry deposition. Controlled wind tunnel experiments have consistently demonstrated that, under idealized conditions and within a certain range of wind speeds, deposition velocity increases with rising wind speed (Freer-Smith et al., 2004). Findings from such experiments have also been used to define dry deposition velocity parameters in the i-Tree Eco model. However, field conditions involve far more complex and variable interactions. Microclimatic variability, microtopography, and plant structural traits collectively influence the actual deposition process, often leading to deviations from model assumptions and controlled experimental outcomes (Cai et al., 2017). In the present case, mean wind speeds remained mostly below 2 m s^{-1}, and in Wufeng, they often fell below 0.5 m s^{-1}. Such low wind conditions limited the extent to which wind could influence deposition velocity. Furthermore, because deposition velocity was calculated as the ratio of flux to concentration, the representativeness of the latter may have exerted greater influence on results. Under stagnant conditions with low wind and poor dispersion, this influence becomes more pronounced, highlighting the greater importance of accurate concentration data over wind speed in dry deposition modeling during high-pollution seasons.

4.4. $PM_{2.5}$ deposition saturation across tree species

The average $PM_{2.5}$ dry deposition distance in this study peaked at approximately 442 h, corresponding to 18.4 d, indicating a potential saturation period for leaf surface accumulation. This timeframe aligns with previous controlled-environment studies, where $PM_{2.5}$ saturation was observed around 16 d (Luo et al., 2020) and total suspended particulate (TSP) between 18 and 21 d (Zhou et al., 2020). Similarly, Liu et al. (2012) found that leaf surface dust in industrial areas reached saturation within 20 d, compared to 24 d in commercial, residential, or rural settings—primarily due to differences in ambient PM concentrations. A *meta*-analysis of 150 studies further suggested that saturation may occur within approximately 10 d (Cai et al., 2017). Such variability reflects the complexity of PM dry deposition dynamics, influenced by ambient PM concentrations and meteorological factors, including wind speed, temperature, and atmospheric turbulence (Liu et al., 2018a). Additionally, interstudy differences in species-specific leaf traits, ambient PM levels, seasonal contexts, and particle size categories can shift the balance between deposition and resuspension, resulting in divergent patterns of dynamic equilibrium (Liu et al., 2013; Zhou et al., 2021). In this study, $PM_{2.5}$ deposition fluxes were normalized against ambient concentrations to derive deposition distance, allowing for the evaluation of interspecific differences in retention efficiency. Species with higher surface roughness, such as *M. azedarach* and *K. henryi*, demonstrated greater $PM_{2.5}$ capture capacity, while smoother-leaved species like *C. camphora* and *P. pinnata* were less effective. Leaf surface roughness is considered a key factor influencing particle adhesion (Song et al., 2015). In particular, observations of leaf microstructures in broadleaved species have shown that a greater number of grooves is associated with enhanced $PM_{2.5}$ accumulation (Chen et al., 2017).

B. javanica, with thick leathery leaves, showed intermediate deposition near the species average, suggesting its utility for $PM_{2.5}$ removal modeling where species-specific data are lacking.

At the Nantun site, the longest recorded deposition time was 780 h; however, deposition distance declined at this point. Given the consistently low average wind speeds across all sites, this decrease was likely driven by small-scale disturbances during prolonged dry deposition periods. In the absence of rainfall-induced washing, short-term gusts or anthropogenic activities can triggered substantial $PM_{2.5}$ resuspension from leaf surfaces (Cai et al., 2017; Xie et al., 2019). Under extreme climatic conditions, extended dry spells are possible. For instance, meteorological data from Nantun indicated that from September to December 2020, dry deposition persisted for over 1723 h, with hourly rainfall consistently below 1 mm (Taiwan Air Quality Monitoring Network). Such conditions may reduce the effectiveness of urban forests in PM removal. In i-Tree Eco simulations, $PM_{2.5}$ removal is calculated by summing hourly dry deposition fluxes, providing high temporal resolution. However, short-term wind events can cause notable resuspension, resulting in negative net fluxes and, in some cases, even model outputs that suggest urban vegetation contributes to air quality deterioration (Parsa et al., 2019). Additionally, in the absence of rainfall exceeding the wash-off threshold, the i-Tree Eco model does not account for deposition saturation, potentially leading to overestimations of long-term $PM_{2.5}$ removal. These findings underscore the need for localized calibration of the model to reflect dynamic processes such as saturation and resuspension under site-specific environmental conditions.

4.5. Biomonitoring applications for atmospheric trace elements

Biomonitoring of trace element enrichment in $PM_{2.5}$ revealed spatial patterns consistent with prior instrument-based measurements in the same urban area, where Fe, Al, and Cr (Kao et al., 2021) or Fe, Al, and Zn (Tsai et al., 2020) were most abundant. Element levels were generally higher in Nantun and Dali and lower in Wufeng, reflecting urbanization intensity. During the late-autumn to early-spring pollution season, northwesterly sea breezes transport industrial emissions from coastal power and steel plants into the study area (Chi & Lin, 2021). Trace element composition, rather than bulk $PM_{2.5}$ mass, captured this gradient more clearly. For example, during T4, Wufeng showed high deposition fluxes but low elemental concentrations, suggesting agricultural sources such as open burning dominated by plant-derived elements (K, Na, Mg) rather than the anthropogenic heavy metals quantified in this study (Akbari et al., 2021). Notably, atmospheric element concentrations were estimated by scaling leaf-surface $PM_{2.5}$ composition to station $PM_{2.5}$ levels. Because inter-site $PM_{2.5}$ differences were small and unmonitored emissions may have occurred in Wufeng, these estimates may not fully capture fine-scale variability. Similar spatial divergence has been observed elsewhere: in Taiyuan, China, $PM_{2.5}$ mass differed by only 10–15 % between urban and rural sites during pollution peaks, yet Ni, Cu, As, and Cd were 1.5–3.2 times higher in urban areas (Liu et al., 2018b). Likewise, Park et al. (2024) showed that metal composition varies significantly by source even when $PM_{2.5}$ mass is comparable. Substantial temporal variation in trace metals was also evident in our study, consistent with Changhua observations where $PM_{2.5}$ varied threefold seasonally, while Pb fluctuated eightfold (Hsu et al., 2016). These findings highlight that $PM_{2.5}$-related health risks depend not only on urbanization but also on meteorology, emission sources, and spatiotemporal variability, underscoring the need to account for trace metal composition in exposure assessments.

Following PCA-based dimensionality reduction and clustering, the first principal component was strongly associated with most trace metals. Previous studies have identified traffic emissions as major sources of Cu, Zn, Pb, bromine (Br), Mn, and Fe (Liu et al., 2020; Yao et al., 2016), with Cu and Zn particularly linked to brake and tire wear (Lopez et al., 2023; Zhao et al., 2021). Hsu et al. (2016) reported that elevated Pb and Cr levels near coal-fired power plants are associated with coal combustion, while Cr, Cu, Zn, As, and Pb are commonly used as tracers of industrial sources (Cai et al., 2021). These findings, together with the present results, suggest that the first component reflects mixed traffic and industrial emissions. The second component, dominated by Mn and Al, likely represents crustal sources, as these elements are abundant in the Earth's crust and commonly used as reference indicators of anthropogenic influence (Hsu et al., 2016; Rahman et al., 2021). Previous studies have also associated Mn and Al with natural weathering and resuspended soil or road dust (Galon-Negru et al., 2019; Liu & Ren, 2019; Liu et al., 2021), supporting the interpretation of a dust-related source. The third component was dominated by Ni, a key indicator of heavy fuel oil combustion, along with vanadium (V), which is frequently used to trace petroleum-based emissions (Bie et al., 2021; Cui et al., 2020; Manousakas et al., 2021). Spatially, Ni levels were relatively higher in Nantun, likely influenced by upwind industrial zones and small boilers in commercial areas such as hotels and restaurants (Ho et al., 2018; Liao et al., 2020). Since 2017, the Taichung City Government has actively promoted the replacement of coal- and oil-fired boilers with cleaner natural gas alternatives. In this study, Ni concentrations were generally low, potentially reflecting the impact of this policy. Nonetheless, the large variability observed in Nantun during T4 and T5 suggests that localized and episodic Ni emissions may still occur.

Overall, urban trees offer multiple advantages for PM and trace metal biomonitoring: (1) they are cost-effective for large-scale, long-term monitoring; (2) sample collection is simple and does not require complex equipment; (3) trees are widely distributed in urban areas and have strong PM-capturing capacity; and (4) they integrate the effects of pollutant levels and meteorological factors, allowing for a more holistic assessment of ambient pollution over time (Rai, 2016; Ram et al., 2015; Wolterbeek, 2002). Their proximity to human activity zones further enhances the representativeness of exposure assessments. However, due to limitations of the passive biomonitoring method used in this study, water-soluble $PM_{2.5}$ fractions and associated metals were not quantified during leaf washing. Future work should integrate active air sampling to improve accuracy and representativeness. Collectively, these findings highlight the effectiveness of urban trees as passive samplers for $PM_{2.5}$-bound toxic elements and underscore the importance of considering both spatial and temporal variability in evaluating exposure risks.

5. Conclusions

This study demonstrates the value of combining field-based measurements and biomonitoring approaches to evaluate $PM_{2.5}$ dry deposition and its modeling performance in urban environments. The i-Tree Eco model effectively reproduced long-term city-scale deposition trends, yet discrepancies at finer spatial and temporal scales highlight the importance of validating its estimates under site-specific conditions. In particular, the representativeness of station-based $PM_{2.5}$ concentrations exerted a greater influence on deposition velocity calculations than wind speed under stagnant, high-pollution conditions, emphasizing the need for improved spatial alignment between monitoring inputs and vegetation sampling sites. Furthermore, the integration of trace metal analysis through leaf-surface biomonitoring provided complementary insights into pollution sources, revealing distinct industrial, traffic, and crustal signatures. Such evidence underscores the role of urban trees as passive samplers for $PM_{2.5}$-bound toxic elements, offering a cost-effective means to capture spatial heterogeneity that conventional monitoring networks often miss. Together, these findings reinforce the necessity of empirical validation, site-specific calibration, and cross-species biomonitoring to enhance the accuracy and applicability of i-Tree Eco in assessing the air-quality regulation services of urban forests.

CRediT authorship contribution statement

Tzu-Hao Su: Conceptualization, Methodology, Investigation, Visualization, Formal Analysis, Writing – original draft, Writing – review &

editing. **Chin-Sheng Lin:** Investigation, Writing – review & editing. **Chiung-Pin Liu:** Resources, Project administration.

Declaration of competing interest

The authors declare that they have no known competing financial interests or personal relationships that could have appeared to influence the work reported in this paper.

Data availability

Data will be made available on request.

References

Adamek, K., Vasan, N., Elshaer, A., English, E., Bitsuamlak, G., 2017. Pedestrian level wind assessment through city development: a study of the financial district in Toronto. Sustain. Cities Soc. 35, 178–190. https://doi.org/10.1016/j.scs.2017.06.004.

Akbari, M.Z., Thepnuan, D., Wiriya, W., Janta, R., Punsompong, P., Hemwan, P., Chantara, S., 2021. Emission factors of metals bound with $PM_{2.5}$ and ashes from biomass burning simulated in an open-system combustion chamber for estimation of open burning emissions. Atmos. Pollut. Res. 12 (3), 13–24. https://doi.org/10.1016/j.apr.2021.01.012.

Askariyeh, M.H., Zietsman, J., Autenrieth, R., 2020. Traffic contribution to $PM_{2.5}$ increment in the near-road environment. Atmos. Environ. 224, 117113. https://doi.org/10.1016/j.atmosenv.2019.117113.

Baldocchi, D.D., 2003. Assessing the eddy covariance technique for evaluating carbon dioxide exchange rates of ecosystems: past, present and future. Glob. Chang. Biol. 9 (4), 479–492. https://doi.org/10.1046/j.1365-2486.2003.00629.x.

Bie, S., Yang, L., Zhang, Y., Huang, Q., Li, J., Zhao, T., Zhang, X., Wang, P., Wang, W., 2021. Source Appointment of PM2.5 in Qingdao Port, East of China. Science of the Total Environment 755, 142456. https://doi.org/10.1016/j.scitotenv.2020.142456.

Cai, A., Zhang, H., Wang, L., Wang, Q., Wu, X., 2021. Source apportionment and health risk assessment of heavy metals in $PM_{2.5}$ in Handan: a typical heavily polluted city in north China. Atmos. 12 (10), 1232. https://doi.org/10.3390/atmos12101232.

Cai, M., Xin, Z., Yu, X., 2017. Spatio-temporal variations in PM leaf deposition: a meta-analysis. Environ. Pollut. 231, 207–218. https://doi.org/10.1016/j.envpol.2017.07.105.

Chen, D., Yan, J., Sun, N., Sun, W., Zhang, W., Long, Y., Yin, S., 2024. Selective capture of $PM_{2.5}$ by urban trees: the role of leaf wax composition and physiological traits in air quality enhancement. J. Hazard. Mater. 478, 135428. https://doi.org/10.1016/j.jhazmat.2024.135428.

Chen, H.W., Chen, C.Y., Chang, T.W., Lin, G.Y., 2023. Spatial-temporal evaluation of $PM_{2.5}$ concentration for health risk reduction strategy development in a basin with different weather patterns. Atmos. Pollut. Res. 14 (10), 101884. https://doi.org/10.1016/j.apr.2023.101884.

Chen, L., Liu, C., Zhang, L., Zou, R., Zhang, Z., 2017. Variation in tree species ability to capture and retain airborne fine particulate matter ($PM_{2.5}$). Sci. Rep. 7 (1), 1–11. https://doi.org/10.1038/s41598-017-03360-1.

Chen, L., Peng, S., Liu, J., Hou, Q., 2012. Dry deposition velocity of total suspended particles and meteorological influence in four locations in Guangzhou. China. Journal of Environmental Sciences 24 (4), 632–639. https://doi.org/10.1016/S1001-0742(11)60805-X.

Chi, W.J., Lin, Y.C., 2021. Investigation of the main $PM_{2.5}$ sources and diffusion patterns and corresponding meteorological conditions by the wavelet analysis approach. Atmos. Pollut. Res. 12 (11), 101222. https://doi.org/10.1016/j.apr.2021.101222.

Cui, Y., Ji, D., Maenhaut, W., Gao, W., Zhang, R., Wang, Y., 2020. Levels and Sources of Hourly PM2.5-Related Elements during the Control Period of the COVID-19 Pandemic at a Rural Site between Beijing and Tianjin. Science of the Total Environment 744, 140840. https://doi.org/10.1016/j.scitotenv.2020.140840.

de Jalón, S.G., Burgess, P., Yuste, J.C., Moreno, G., Graves, A., Palma, J., Crous-Duran, J., Kay, S., Chiabai, A., 2019. Dry deposition of air pollutants on trees at regional scale: a case study in the Basque Country. Agric. For. Meteorol. 278, 107648. https://doi.org/10.1016/j.agrformet.2019.107648.

Dzierżanowski, K., Popek, R., Gawrońska, H., Sæbø, A., Gawroński, S.W., 2011. Deposition of particulate matter of different size fractions on leaf surfaces and in waxes of urban forest species. Int. J. Phytorem. 13 (10), 1037–1046. https://doi.org/10.1080/15226514.2011.552929.

Fang, C., Zhang, Z., Jin, M., Zou, P., Wang, J., 2017. Pollution characteristics of $PM_{2.5}$ aerosol during haze periods in Changchun. China. Aerosol and Air Quality Research 17 (4), 888–895. https://doi.org/10.4209/aaqr.2016.09.0407.

Fares, S., Conte, A., Alivernini, A., Chianucci, F., Grotti, M., Zappitelli, I., Petrella, F., Corona, P., 2020. Testing Removal of Carbon Dioxide, ozone, and Atmospheric Particles by Urban Parks in Italy. Environ. Sci. Tech. 54 (23), 14910–14922. https://doi.org/10.1021/acs.est.0c04740.

Feng, S., Gao, D., Liao, F., Zhou, F., Wang, X., 2016. The health effects of ambient $PM_{2.5}$ and potential mechanisms. Ecotoxicol. Environ. Saf. 128, 67–74. https://doi.org/10.1016/j.ecoenv.2016.01.030.

Freer-Smith, P.H., El-Khatib, A.A., Taylor, G., 2004. Capture of particulate pollution by trees: a comparison of species typical of semi-arid areas (*Ficus nitida* and *Eucalyptus globulus*) with European and north American species. Water Air Soil Pollut. 155 (1–4), 173–187. https://doi.org/10.1023/B:WATE.0000026521.99552.fd.

Gaglio, M., Pace, R., Muresan, A.N., Grote, R., Castaldelli, G., Calfapietra, C., Fano, E.A., 2022. Species-specific efficiency in $PM_{2.5}$ removal by urban trees: from leaf measurements to improved modeling estimates. Sci. Total Environ. 844, 157131. https://doi.org/10.1016/j.scitotenv.2022.157131.

Galon-Negru, A.G., Olariu, R.I., Arsene, C., 2019. Size-resolved measurements of $PM_{2.5}$ water-soluble elements in Iasi, north-eastern Romania: Seasonality, source apportionment and potential implications for human health. Sci. Total Environ. 695, 133839. https://doi.org/10.1016/j.scitotenv.2019.133839.

Gonzalez-Sosa, E., Braud, I., Piña, R.B., Loza, C.A.M., Salinas, N.M.R., Chavez, C.V., 2017. A methodology to quantify ecohydrological services of street trees. Ecohydrol. Hydrobiol. 17 (3), 190–206. https://doi.org/10.1016/j.ecohyd.2017.06.004.

Han, D., Shen, H., Duan, W., Chen, L., 2020. A review on particulate matter removal capacity by urban forests at different scales. Urban For. Urban Green. 48, 126565. https://doi.org/10.1016/j.ufug.2019.126565.

Hirabayashi, S., Kroll, C. N., Nowak, D. J., & Endreny, T. A. (2022). i-Tree eco dry deposition model descriptions. Retrieved July 5, 2025, from https://www.itreetools.org/documents/60/i-Tree_Eco_Dry_Deposition_Model_Descriptions_V1.5.pdf.

Ho, W.Y., Tseng, K.H., Liou, M.L., Chan, C.C., Wang, C.H., 2018. Application of Positive Matrix Factorization in the Identification of the Sources of PM2.5 in Taipei City. International Journal of Environmental Research and Public Health 15 (7), 1305. https://doi.org/10.3390/ijerph15071305.

Hofman, J., Wuyts, K., Van Wittenberghe, S., Brackx, M., Samson, R., 2014. Reprint of on the link between biomagnetic monitoring and leaf-deposited dust load of urban trees: relationships and spatial variability of different particle size fractions. Environ. Pollut. 192, 285–294. https://doi.org/10.1016/j.envpol.2014.05.006.

Hsu, C.Y., Chiang, H.C., Lin, S.L., Chen, M.J., Lin, T.Y., Chen, Y.C., 2016. Elemental characterization and source apportionment of PM_{10} and $PM_{2.5}$ in the western coastal area of central Taiwan. Sci. Total Environ. 541, 1139–1150. https://doi.org/10.1016/j.scitotenv.2015.09.122.

Kao, C.-L., Fang, G.C., Gao, W.S., Zhuang, Y.J., 2021. Concentrations, sizes distributions, and seasonal variations of ambient air pollutants (particulates, trace metals) in Daya/Xitun District, Taichung, Central Taiwan: a case study at Taichung Science Park. J. Environ. Sci. Health A 1–11. https://doi.org/10.1080/10934529.2021.1936988.

Kermani, M., Jafari, A.J., Gholami, M., Arfaeinia, H., Shahsavani, A., Fanaei, F., 2021. Characterization, possible sources and health risk assessment of $PM_{2.5}$-bound Heavy Metals in the most industrial city of Iran. J. Environ. Health Sci. Eng. 1–13. https://doi.org/10.1007/s40201-020-00589-3.

Kong, S., Yan, Q., Zheng, H., Liu, H., Wang, W., Zheng, S., Yang, G., Zheng, M., Wu, J., Qi, S., 2018. Substantial reductions in ambient PAHs pollution and lives saved as a co-benefit of effective long-term $PM_{2.5}$ pollution controls. Environ. Int. 114, 266–279. https://doi.org/10.1016/j.envint.2018.03.002.

Liang, D., Ma, C., Wang, Y.Q., Wang, Y.J., Zhao, C.X., 2016. Quantifying $PM_{2.5}$ capture capability of greening trees based on leaf factors analyzing. Environ. Sci. Pollut. Res. 23 (21), 21176–21186. https://doi.org/10.1007/s11356-016-7687-9.

Liao, H.T., Chang, J.C., Tsai, T.T., Tsai, S.W., Chou, C.C.K., Wu, C.F., 2020. Vertical distribution of source apportioned $PM_{2.5}$ using particulate-bound elements and polycyclic aromatic hydrocarbons in an urban area. J. Eposure Sci. Environ. Epidemiol. 30 (4), 659–669. https://doi.org/10.1038/s41370-019-0153-2.

Lin, J., Kroll, C.N., Nowak, D.J., Greenfield, E.J., 2019. A review of urban forest modeling: Implications for management and future research. Urban For. Urban Green. 43. https://doi.org/10.1016/j.ufug.2019.126366.

Liu, J., Yan, G., Wu, Y., Wang, Y., Zhang, Z., Zhang, M., 2018a. Wetlands with greater degree of urbanization improve $PM_{2.5}$ removal efficiency. Chemosphere 207, 601–611. https://doi.org/10.1016/j.chemosphere.2018.05.131.

Liu, K., Ren, J., 2019. Characteristics, sources and health risks of $PM_{2.5}$-bound potentially toxic elements in the northern rural China. Atmos. Pollut. Res. 10 (5), 1621–1626. https://doi.org/10.1016/j.apr.2019.06.002.

Liu, K., Shang, Q., Wan, C., Song, P., Ma, C., Cao, L., 2018b. Characteristics and sources of heavy metals in $PM_{2.5}$ during a typical haze episode in rural and urban areas in Taiyuan. China. Atmosphere 9 (1), 2. https://doi.org/10.3390/atmos9010002.

Liu, L., Guan, D., Peart, M., 2012. The morphological structure of leaves and the dust-retaining capability of afforested plants in urban Guangzhou, South China. Environ. Sci. Pollut. Res. 19 (8), 3440–3449. https://doi.org/10.1007/s11356-012-0876-2.

Liu, L., Guan, D., Peart, M., Wang, G., Zhang, H., Li, Z., 2013. The dust retention capacities of urban vegetation—a case study of Guangzhou, South China. Environ. Sci. Pollut. Res. 20 (9), 6601–6610. https://doi.org/10.1007/s11356-013-1648-3.

Liu, L., Liu, Y.S., Wen, W., Liang, L.L., Ma, X., Jiao, J., Guo, K., 2020. Source identification of trace elements in $PM_{2.5}$ at a rural site in the North China Plain. Atmos. 11 (2), 179. https://doi.org/10.3390/atmos11020179.

Liu, Y., Yang, Z., Liu, Q., Qi, X., Qu, J., Zhang, S., Wang, X., Jia, K., Zhu, M., 2021. Study on chemical components and sources of $PM_{2.5}$ during heavy air pollution periods at a suburban site in Beijing of China. Atmos. Pollut. Res. 12 (4), 188–199. https://doi.org/10.1016/j.apr.2021.03.006.

Lopez, B., Wang, X., Chen, L.W.A., Ma, T., Mendez-Jimenez, D., Cobb, L.C., Jung, H., 2023. Metal contents and size distributions of brake and tire wear particles dispersed in the near-road environment. Sci. Total Environ. 883, 163561. https://doi.org/10.1016/j.scitotenv.2023.163561.

Lu, S., Yang, X., Li, S., Chen, B., Jiang, Y., Wang, D., Xu, L., 2018. Effects of plant leaf surface and different pollution levels on $PM_{2.5}$ adsorption capacity. Urban For. Urban Green. 34, 64–70. https://doi.org/10.1016/j.ufug.2018.05.006.

Luo, J., Niu, Y., Zhang, Y., Zhang, M., Tian, Y., Zhou, X., 2020. Dynamic analysis of retention $PM_{2.5}$ by plant leaves in rainfall weather conditions of six tree species.

Energy Sources Part A 42 (8), 1014–1025. https://doi.org/10.1080/15567036.2019.1602212.

Manousakas, M., Diapouli, E., Belis, C., Vasilatou, V., Gini, M., Lucarelli, F., Querol, X., Eleftheriadis, K., 2021. Quantitative assessment of the variability in chemical profiles from source apportionment analysis of PM_{10} and $PM_{2.5}$ at different sites within a large metropolitan area. Environ. Res. 192, 110257. https://doi.org/10.1016/j.envres.2020.110257.

Mohan, S.M., 2016. An overview of particulate dry deposition: measuring methods, deposition velocity and controlling factors. Int. J. Environ. Sci. Technol. 13 (1), 387–402. https://doi.org/10.1007/s13762-015-0898-7.

Mori, J., Hanslin, H.M., Burchi, G., Saebo, A., 2015. Particulate matter and element accumulation on coniferous trees at different distances from a highway. Urban For. Urban Green. 14 (1), 170–177. https://doi.org/10.1016/j.ufug.2014.09.005.

Norouzi, S., Khademi, H., Cano, A.F., Acosta, J.A., 2015. Using plane tree leaves for biomonitoring of dust borne heavy metals: a case study from Isfahan, Central Iran. Ecol. Ind. 57, 64–73. https://doi.org/10.1016/j.ecolind.2015.04.011.

Nowak, D.J., Hirabayashi, S., Bodine, A., Hoehn, R., 2013. Modeled $PM_{2.5}$ removal by trees in ten U.S. cities and associated health effects. Environ. Pollut. 178, 395–402. https://doi.org/10.1016/j.envpol.2013.03.050.

Nowak, D.J., 2023. In: Improved Air Quality and Other Services from Urban Trees and Forests. Engineering and Ecosystems. Springer, Cham. https://doi.org/10.1007/978-3-031-35692-6_10.

Pace, R., Biber, P., Pretzsch, H., Grote, R., 2018. Modeling ecosystem services for park trees: Sensitivity of i-tree eco simulations to light exposure and tree species classification. Forests 9 (2), 89. https://doi.org/10.3390/f9020089.

Pace, R., Guidolotti, G., Baldacchini, C., Pallozzi, E., Grote, R., Nowak, D.J., Calfapietra, C., 2021. Comparing i-tree Eco estimates of particulate matter deposition with leaf and canopy measurements in an urban Mediterranean holm oak forest. Environ. Sci. Tech. 55 (10), 6613–6622. https://doi.org/10.1021/acs.est.0c07679.

Pallozzi, E., Guidolotti, G., Mattioni, M., Calfapietra, C., 2020. Particulate matter concentrations and fluxes within an urban park in Naples. Environ. Pollut. 266 (Pt 3), 115134. https://doi.org/10.1016/j.envpol.2020.115134.

Park, S.Y., Jeon, J.I., Jung, J.Y., Yoon, S.W., Kwon, J., Lee, C.M., 2024. $PM_{2.5}$ and heavy metals in urban and agro-industrial areas: health risk assessment considerations. Asian J. Atmos. Environ. 18 (1), 16. https://doi.org/10.1007/s44273-024-00037-w.

Parsa, V.A., Salehi, E., Yavari, A.R., van Bodegom, P.M., 2019. An improved method for assessing mismatches between supply and demand in urban regulating ecosystem services: a case study in Tabriz. Iran. Plos One 14 (8), e0220750. https://doi.org/10.1371/journal.pone.0220750.

Peachey, C.J., Sinnett, D., Wilkinson, M., Morgan, G.W., Freer-Smith, P.H., Hutchings, T. R., 2009. Deposition and solubility of airborne metals to four plant species grown at varying distances from two heavily trafficked roads in London. Environ. Pollut. 157 (8–9), 2291–2299. https://doi.org/10.1016/j.envpol.2009.03.032.

Popek, R., Gawrońska, H., Wrochna, M., Gawroński, S.W., Sæbø, A., 2013. Particulate matter on foliage of 13 woody species: deposition on surfaces and phytostabilisation in waxes–a 3-year study. Int. J. Phytorem. 15 (3), 245–256. https://doi.org/10.1080/15226514.2012.694498.

Rahman, M.A., Armson, D., Ennos, A., 2015. A comparison of the growth and cooling effectiveness of five commonly planted urban tree species. Urban Ecosystems 18 (2), 371–389. https://doi.org/10.1007/s11252-014-0407-7.

Rahman, M.S., Bhuiyan, S.S., Ahmed, Z., Saha, N., Begum, B.A., 2021. Characterization and source apportionment of elemental species in $PM_{2.5}$ with especial emphasis on seasonal variation in the capital city "Dhaka". Bangladesh. Urban Climate 36, 100804. https://doi.org/10.1016/j.uclim.2021.100804.

Rai, P.K., 2016. Impacts of particulate matter pollution on plants: Implications for environmental biomonitoring. Ecotoxicol. Environ. Saf. 129, 120–136. https://doi.org/10.1016/j.ecoenv.2016.03.012.

Ram, S., Majumder, S., Chaudhuri, P., Chanda, S., Santra, S., Chakraborty, A., Sudarshan, M., 2015. A review on air pollution monitoring and management using plants with special reference to foliar dust adsorption and physiological stress responses. Crit. Rev. Environ. Sci. Technol. 45 (23), 2489–2522. https://doi.org/10.1080/10643389.2015.1046775.

Riley, C.B., Herms, D.A., Gardiner, M.M., 2018. Exotic trees contribute to urban forest diversity and ecosystem services in inner-city Cleveland, OH. Urban For. Urban Green. 29, 367–376. https://doi.org/10.1016/j.ufug.2017.01.004.

Riondato, E., Pilla, F., Basu, A.S., Basu, B., 2020. Investigating the effect of trees on urban quality in Dublin by combining air monitoring with i-tree Eco model. Sustain. Cities Soc. 61, 102356. https://doi.org/10.1016/j.scs.2020.102356.

Sæbø, A., Popek, R., Nawrot, B., Hanslin, H.M., Gawronska, H., Gawronski, S.W., 2012. Plant species differences in particulate matter accumulation on leaf surfaces. Sci. Total Environ. 427–428, 347–354. https://doi.org/10.1016/j.scitotenv.2012.03.084.

Santunione, G., Barbieri, A., Sgarbi, E., 2024. Analysis of particulate matter (PM) trapped by four different plant species in an urban forest: Quantification and characterization. Trees, Forests and People 16, 100585. https://doi.org/10.1016/j.tfp.2024.100585.

Selmi, W., Weber, C., Riviere, E., Blond, N., Mehdi, L., Nowak, D., 2016. Air pollution removal by trees in public green spaces in Strasbourg city, France. Urban For. Urban Green. 17, 192–201. https://doi.org/10.1016/j.ufug.2016.04.010.

Sgrigna, G., Saebo, A., Gawronski, S., Popek, R., Calfapietra, C., 2015. Particulate Matter deposition on *Quercus ilex* leaves in an industrial city of central Italy. Environ. Pollut. 197, 187–194. https://doi.org/10.1016/j.envpol.2014.11.030.

Simon, E., Braun, M., Vidic, A., Bogyo, D., Fabian, I., Tothmeresz, B., 2011. Air pollution assessment based on elemental concentration of leaves tissue and foliage dust along an urbanization gradient in Vienna. Environ. Pollut. 159 (5), 1229–1233. https://doi.org/10.1016/j.envpol.2011.01.034.

Song, Y., Maher, B.A., Li, F., Wang, X., Sun, X., Zhang, H., 2015. Particulate matter deposited on leaf of five evergreen species in Beijing, China: source identification and size distribution. Atmos. Environ. 105, 53–60. https://doi.org/10.1016/j.atmosenv.2015.01.032.

Sosa, B.S., Porta, A., Lerner, J.E.C., Noriega, R.B., Massolo, L., 2017. Human health risk due to variations in PM_{10}–$PM_{2.5}$ and associated PAHs levels. Atmos. Environ. 160, 27–35. https://doi.org/10.1016/j.atmosenv.2017.04.004.

Tsai, P.-J., Young, L.H., Hwang, B.F., Lin, M.Y., Chen, Y.C., Hsu, H.T., 2020. Source and health risk apportionment for $PM_{2.5}$ collected in Sha-Lu area. Taiwan. Atmospheric Pollution Research 11 (5), 851–858. https://doi.org/10.1016/j.apr.2020.01.013.

Vos, P.E., Maiheu, B., Vankerkom, J., Janssen, S., 2013. Improving local air quality in cities: to tree or not to tree? Environ. Pollut. 183, 113–122. https://doi.org/10.1016/j.envpol.2012.10.021.

Wang, H., Shi, H., Li, Y., Yu, Y., Zhang, J., 2013. Seasonal variations in leaf capturing of particulate matter, surface wettability and micromorphology in urban tree species. Frontiers of Environmental Science and Engineering 7 (4), 579–588. https://doi.org/10.1007/s11783-013-0524-1.

Wang, J., Endreny, T.A., Nowak, D.J., 2008. Mechanistic simulation of tree effects in an urban water balance model 1. JAWRA Journal of the American Water Resources Association 44 (1), 75–85. https://doi.org/10.1111/j.1752-1688.2007.00139.x.

Wang, X., Wei, W., Cheng, S., Li, J., Zhang, H., Lv, Z., 2018. Characteristics and classification of $PM_{2.5}$ pollution episodes in Beijing from 2013 to 2015. Sci. Total Environ. 612, 170–179. https://doi.org/10.1016/j.scitotenv.2017.08.206.

Wolterbeek, B., 2002. Biomonitoring of trace element air pollution: principles, possibilities and perspectives. Environ. Pollut. 120 (1), 11–21. https://doi.org/10.1016/S0269-7491(02)00124-0.

Wu, C.F., Lin, H.I., Ho, C.C., Yang, T.H., Chen, C.C., Chan, C.C., 2014. Modeling horizontal and vertical variation in intraurban exposure to $PM_{2.5}$ concentrations and compositions. Environ. Res. 133, 96–102. https://doi.org/10.1016/j.envres.2014.04.038.

Wu, J., Wang, Y., Qiu, S., Peng, J., 2019. Using the modified i-tree Eco model to quantify air pollution removal by urban vegetation. Sci. Total Environ. 688, 673–683. https://doi.org/10.1016/j.scitotenv.2019.05.437.

Xie, C., Yan, L., Liang, A., Che, S., 2019. Understanding the washoff processes of $PM_{2.5}$ from leaf surfaces during rainfall events. Atmos. Environ. 214, 116844. https://doi.org/10.1016/j.atmosenv.2019.116844.

Xie, Y., Zhao, B., Zhao, Y., Luo, Q., Wang, S., Bai, S., 2017. Reduction in population exposure to $PM_{2.5}$ and cancer risk due to $PM_{2.5}$-bound PAHs exposure in Beijing, China during the APEC meeting. Environ. Pollut. 225, 338–345. https://doi.org/10.1016/j.envpol.2017.02.059.

Xu, X., Xia, J., Gao, Y., Zheng, W., 2020. Additional focus on particulate matter wash-off events from leaves is required: a review of studies of urban plants used to reduce airborne particulate matter pollution. Urban For. Urban Green. 48, 126559. https://doi.org/10.1016/j.ufug.2019.126559.

Yao, L., Yang, L., Yuan, Q., Yan, C., Dong, C., Meng, C., Sui, X., Yang, F., Lu, Y., Wang, W., 2016. Sources apportionment of $PM_{2.5}$ in a background site in the North China Plain. Sci. Total Environ. 541, 590–598. https://doi.org/10.1016/j.scitotenv.2015.09.123.

Zhang, W., Wang, B., Niu, X., 2017. Relationship between leaf surface characteristics and particle capturing capacities of different tree species in Beijing. Forests 8 (3), 92. https://doi.org/10.3390/f8030092.

Zhang, X., Lyu, J., Han, Y., Sun, N., Sun, W., Li, J., Liu, C., & Yin, S. (2020). Effects of the leaf functional traits of coniferous and broadleaved trees in subtropical monsoon regions on $PM_{2.5}$ dry deposition velocities. Environmental Pollution, 265(Pt B), 114845. Doi:10.1016/j.envpol.2020.114845.

Zhao, X., Li, Z., Wang, D., Tao, Y., Qiao, F., Lei, L., Huang, J., Ting, Z., 2021. Characteristics, source apportionment and health risk assessment of heavy metals exposure via household dust from six cities in China. Sci. Total Environ. 762, 143126. https://doi.org/10.1016/j.scitotenv.2020.143126.

Zheng, X.B., Xu, X.J., Yekeen, T.A., Zhang, Y.L., Chen, A.M., Kim, S.S., Dietrich, K.N., Ho, S.M., Lee, S.A., Reponen, T., Huo, X., 2016. Ambient air heavy metals in $PM_{2.5}$ and potential human health risk assessment in an informal electronic-waste recycling site of China. Aerosol Air Qual. Res. 16 (2), 388–397. https://doi.org/10.4209/aaqr.2014.11.0292.

Zhou, M., Wang, X., Lin, X., Yang, S., Zhang, J., Chen, J., 2020. Automobile exhaust particles retention capacity assessment of two common garden plants in different seasons in the Yangtze River Delta using open-top chambers. Environ. Pollut. 263, 114560. https://doi.org/10.1016/j.envpol.2020.114560.

Zhou, Y., Chen, C., Lu, T., Zhang, J., Chen, J., 2021. Season impacts on estimating plant's particulate retention: Field experiments and meta-analysis. Chemosphere 132570. https://doi.org/10.1016/j.chemosphere.2021.132570.